PCCP

Properties of perhalogenated {*closo*-B_{10}} and {*closo*-B_{11}} multiply charged anions and a critical comparison with {*closo*-B_{12}} in the gas and condensed phases

Journal:	*Physical Chemistry Chemical Physics*
Manuscript ID	CP-ART-08-2018-005313.R1
Article Type:	Paper
Date Submitted by the Author:	24-Oct-2018
Complete List of Authors:	Warneke, Jonas; Universität Bremen, Fachbereich 2 (Chemie/Biologie) Konieczka, Szymon; Julius-Maximilians-Universität Würzburg, Institut für Anorganische Chemie Hou, Gao-Lei; Eidgenossische Technische Hochschule Zurich Departement Chemie und Angewandte Biowissenschaften, Laboratory of Physical Chemistry Aprà, Edoardo; Pacific Northwest National Lab, EMSL Kerpen, Christoph; Julius-Maximilians-Universität Würzburg, Institut für Anorganische Chemie Keppner, Fabian; Julius-Maximilians-Universität Würzburg, Institut für Anorganische Chemie Schäfer, Thomas; Julius-Maximilians-Universität Würzburg, Institut für Anorganische Chemie Deckert, Michael; Julius-Maximilians-Universität Würzburg, Institut für Anorganische Chemie Yang, Zheng; Pacific Northwest National Laboratory, Physical Sciences Division Bylaska, Eric; Pacific Northwest National Laboratory, Johnson, Grant; Pacific Northwest National Laboratory, Chemical Physics and Analysis Laskin, Julia; Purdue University, Chemistry; Department of Chemistry, Purdue University Xantheas, Sotiris; Pacific Northwest National Laboratory, Physical Sciences Division Wang, Xue-Bin; Pacific Northwest National Laboratory, Physical Sciences Division Finze, Maik; Julius-Maximilians-Universität Würzburg, Institut für Anorganische Chemie

Journal Name

ARTICLE

Properties of perhalogenated {*closo*-B_{10}} and {*closo*-B_{11}} multiply charged anions and a critical comparison with {*closo*-B_{12}} in the gas and the condensed phase

Received 00th January 20xx,
Accepted 00th January 20xx

DOI: 10.1039/x0xx00000x

www.rsc.org/

Jonas Warneke,*[a] Szymon Z. Konieczka,[b] Gao-Lei Hou,[a] Edoardo Aprà,[c] Christoph Kerpen,[b] Fabian Keppner,[b] Thomas C. Schäfer,[b] Michael Deckert,[b] Zheng Yang,[a] Eric J. Bylaska,[c] Grant E. Johnson,[a] Julia Laskin,[d] Sotiris S. Xantheas,[e,f] Xue-Bin Wang,[a] Maik Finze*[b]

closo-Borate anions [*closo*-B_nX_n]$^{2-}$ are part of the most famous textbook examples of polyhedral compounds. Substantial differences in their reactivity and interactions with other compounds depending on the substituent *X* and cluster size *n* have been recognized, which favors specific *closo*-borates for different applications in cancer treatment, chemical synthesis, and materials science. Surprisingly, a fundamental understanding of the molecular properties underlying these differences is lacking. Here, we report our study comparing the electronic structure and reactivity of *closo*-borate anions [*closo*-B_nX_n]$^{2-}$ (*X* = Cl, Br, I, *n* = 10, 11, 12 in all combinations) in the gas phase and in solution. We investigated the free dianions and the ion pairs [*n*Bu_4N]$^+$[*closo*-B_nX_n]$^{2-}$ by gas phase anion photoelectron spectroscopy accompanied by theoretical investigations. Strong similarities in electronic structure for *n* = 10 and 11 were observed, while *n* = 12 clusters are different. A systematic picture of the development in electronic stability along the dimension *X* is derived. Collision induced dissociation shows that fragmentation of the free dianions is mainly dependent on the substituent *X* and gives access to a large variety of boron-rich molecular ions. Fragmentation of the ion pair depends strongly on *n*. The results reflect the high chemical stability of cluster with *n* = 10 and 12, while those with *n* = 11 are much easier prone to dissociation. We bridge our study to the condensed phase by performing comparative electrochemistry and reactivity studies on *closo*-borates in solution. The trends found at the molecular level are also reflected in the condensed-phase properties. We discuss how the gas phase values allow to evaluate the influence of the condensed phase on the electronic stability of *closo*-borates. A synthetic method via an oxidation/chlorination reaction yielding [*closo*-$B_{10}Cl_{10}$]$^{2-}$ from highly chlorinated {*closo*-B_{11}} clusters is introduced, which underlines the intrinsically high reactivity of the {*closo*-B_{11}} cage.

Introduction

Boron chemistry has been the subject of chemists' curiosity since the early discoveries of A. Stock[1] due to the often reported strong differences from the intuitively understandable and well explored carbon chemistry. The groundbreaking work on the geometric and electronic structures of boron hydrides by W. N. Lipscomb[2] and the fascinating synthetic developments in the 1960's that made boron clusters available, for the first time, marked the beginning of broad and general studies on this class of compounds. Nowadays, *closo*-borate anions with the general formula [*closo*-B_nX_n]$^{2-}$ (*X* = H, halogen) are described in every basic inorganic chemistry textbook as important representatives of boron compounds. In this series, the *closo*-dodecaborate anion (*n* = 12) is the most studied and best understood species[3] followed by the *closo*-decaborate anion (*n* = 10),[4] because of their high stabilities and the fact that their salts are easily accessible. In contrast, other members of the series of *closo*-borate anions possess much lower chemical stabilities with the parent 11-vertex *closo*-cluster [*closo*-$B_{11}H_{11}$]$^{2-}$ being a representative example due to its significantly higher reactivity.[5] This higher and often unusual reactivity is exemplified by the fluxionality of the {*closo*-B_{11}} cage that results in rapid interconversion of the eleven boron vertices.[5b,5c,6] *closo*-Borates have been explored for almost half a century in the context of cancer treatment (e.g. boron neutron capture therapy, BNCT[7]) and different areas of materials science (e.g. battery technologies[8]).[9] The halogenated 12-vertex derivatives [*closo*-$B_{12}X_{12}$]$^{2-}$ [10] and [R_3N-*closo*-$B_{12}X_{11}$]$^-$ (*R* = H, alkyl, *X* = halogen)[11] gained significant attention in the last decade as

[a] *Physical Sciences Division, Pacific Northwest National Laboratory, 902 Battelle Boulevard, P.O. Box 999, MSIN K8-88, WA, 99352, USA, E-mail: Jonas.Warneke@pnnl.gov*
[b] *Julius-Maximilians-Universität Würzburg, Institute for Inorganic Chemistry, Institute for Sustainable Chemistry & Catalysis with Boron (ICB), Am Hubland, 97074 Würzburg, Germany, E-mail: maik.finze@uni-wuerzburg.de*
[c] *Environmental Molecular Sciences Laboratory, Pacific Northwest National Laboratory, P. O. Box 999, Richland, WA 99352, USA*
[d] *Department of Chemistry, Purdue University, West Lafayette, IN 47907, USA*
[e] *Advanced Computing, Mathematics and Data Division, Pacific Northwest National Laboratory, 902 Battelle Boulevard, P.O. Box 999, MS K1-83, WA, 99352, USA*
[f] *Department of Chemistry, University of Washington, Seattle, WA, 98195, USA*

weakly coordinating anions[12] due to their exceptional electronic stability and chemical inertness, which enables applications[12] in synthesis,[10a] catalysis,[13] crystal engineering,[14] and electrochemical devices.[15] Furthermore, radicals of the type [*closo*-$B_{11}X_{11}$]$^{\bullet-}$ and R_3N-*closo*-$B_{12}X_{11}^{\bullet}$ are highly interesting species used as boron-based spin carriers and as strong oxidizers.[16]

Intensive fundamental research during the last two years with a focus on the 12-vertex cluster resulted in several physicochemical records. For example, [*closo*-$B_{12}(CN)_{12}]^{2-}$ and [*closo*-$B_{12}(BO)_{12}]^{2-}$ were predicted to be the most electronically stable dianions based on calculations,[17] [*closo*-$B_{12}X_{12}]^{2-}$ (*X* = Cl, Br, I) were shown to be "superchaotropic" anions that lie beyond the traditional Hofmeister scale,[18] while [*closo*-$B_{12}F_{12}]^{2-}$ showed exceptionally strong interactions with neutral molecules in the gas phase,[19] and the anion [*closo*-$B_{12}Cl_{11}]^{-}$ was demonstrated to exhibit super-electrophilic behavior by spontaneously binding of the noble gases Kr and Xe.[20] Despite the well-known differences in the reactivity of *closo*-borate anions with e.g. *n* = 10, 11, and 12,[3-4,5b] it has been well established that there are remarkable differences in the molecular interactions with different *closo*-borates as a function of both cluster size *n* and substituent *X*. In the context of medical applications, it has been shown that deca- and dodecaborate (*n* = 10, 12) derivatives differ considerably in their metabolic pathways[7a,21] and a series of halogenated dodecaborate clusters (same *n* but different *X*) showed different biochemical activity (e.g. different interactions with liposomes).[22] The potential of this class of compounds to provide precisely-controlled interactions with other molecules, not only in medicinal applications but also in various fields of materials science, may only be fully exploited if the properties of the ions are understood at the fundamental molecular level. Such understanding could form the basis for the rational design of new tumor targeting drugs for inoperable cancers containing boron clusters[23] and for tailoring the properties of different functional materials that have been recently developed based on *closo*-borates.[24]

To obtain insights into the intrinsic physical and chemical properties of [*closo*-$B_nX_n]^{2-}$ ions all combinations of *n* = 10, 11, 12 with *X* = Cl, Br, I were prepared (see Figure 1 for comparison of the boron scaffold). First, we explored these ions in the gas phase where they can be studied without the complications of condensed phase effects (e.g. solvent shells and counter ions). Their electronic structures were explored by photoelectron spectroscopy (PES) and high-level electronic structure calculations while their fragmentation pathways were probed using collision-induced dissociation (CID). Additionally, we investigated the influence of a single counter ion on both the PES spectra and fragmentation pathways in the gas phase. Finally, comparative electrochemical measurements were conducted to explore the reactivity of these species in the condensed phase. The goal of the present study is to evaluate the effect of both *n* and *X* in [*closo*-$B_nX_n]^{2-}$ ions on their electronic structure, electrochemical stability as well as reactivity, and to bridge the gap between their gas-phase ion chemistry and their condensed-phase properties.

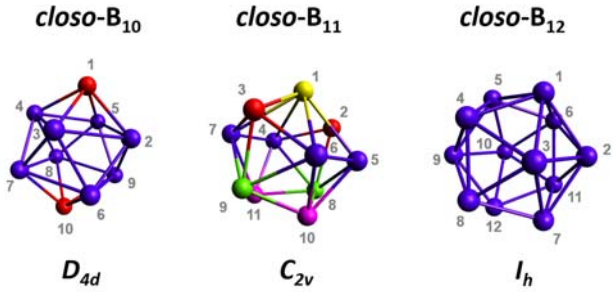

Figure 1 Boron scaffold of *closo*-deca-, *closo*-undeca- and *closo*-dodecaborates, showing the atom numbering (grey) and the molecular point groups (bottom). Symmetry equivalent atoms are shown in the same color for each case. {*closo*-B_{10}} cluster: B1 and B10 have an inner cluster connectivity of 4, while all other B atoms have an inner cluster connectivity of 5. {*closo*-B_{11}} cluster: B1 has an inner cluster connectivity of 6, B2 and B3 of 4, and all other B atoms of 5. {*closo*-B_{12}} cluster: all B atoms have an inner cluster connectivity of 5.

Results and Discussion

A. Properties of Isolated Anions

A.1. Electronic stability of [*closo*-$B_nX_n]^{2-}$: In contrast to the condensed phase, small stable multiply charged anions (MCAs) in the gas phase are typically exotic species. While large multiply charges macromolecules are often observed in mass spectrometry experiments because charged sites are well separated, many small molecular gas phase dianions either emit an electron or undergo fragmentation accompanied by charge separation in the absence of the stabilizing effects of counter ions and solvent molecules.[25] Small but intrinsically stable multiply charged anions (MCAs) have, therefore, been investigated by theoreticians and experimentalists alike for decades.[17a,26] Among them, dodecaborate anions [*closo*-$B_{12}X_{12}]^{2-}$ are representatives of gas phase stable MCAs. Previous theoretical investigations for *X* = H indicated that *closo*-boron clusters of the series [*closo*-$B_nH_n]^{2-}$ are unstable with respect to electron emission for *n* < 12,[26d,27] a fact that has been confirmed by us experimentally. Specifically, neither [*closo*-$B_{11}H_{11}]^{2-}$ nor [*closo*-$B_{10}H_{10}]^{2-}$ were detected in our mass spectrometry experiments. Instead, the *closo*-boron clusters were observed as singly charged (1-) radical species, viz. [*closo*-$B_nH_n]^{\bullet-}$ (*n* = 10, 11). In contrast, the [*closo*-$B_{12}H_{12}]^{2-}$ ion was detected as a stable dianion in the gas phase. Smaller (*n* < 12) *closo*-borate anions with electronically stabilizing substituents have also been the subject of earlier theoretical studies.[28] However, to the best of our knowledge, no experimental investigation of these species has been reported to date. For this reason, we studied perhalogenated {*closo*-B_{10}} and {*closo*-B_{11}} dianions with electrospray ionization mass spectrometry and photoelectron spectroscopy (PES). Figure 2 shows the PES spectra of [*closo*-$B_{10}X_{10}]^{2-}$ and [*closo*-$B_{11}X_{11}]^{2-}$ (*X* = Cl, Br, I) and for comparison the previously published spectra of the corresponding {*closo*-B_{12}} derivatives.[29] Quantitative values describing their electronic stability, vertical detachment energies (VDEs) and adiabatic detachment energies (ADE), were determined by measuring the first maximum (dashed line) and the onset of the first spectral band (dotted line), respectively, and are given in Table 1 (see details for interpretation of PES spectra in SI1). Deca- and undecaborate anions (*n* = 10, 11) exhibit very similar values for VDEs and ADEs, but are significantly

Table 1 Calculated (DFT/PBE0) and measured (PES) vertical (VDEs; eV) and adiabatic detachment energies (ADEs; eV). Experimental values for VDEs and ADEs have uncertainties of ±0.05 and ±0.1 eV, respectively. Values for the dodecaborate anions (n = 12) are taken from the literature.[29] A comparison with Hatree Fock results can be found in SI2.

	VDE			ADE		
anion	PBE0	PES	Difference (PES-PBE0)	PBE0	PES	Difference (PES-PBE0)
[*closo*-$B_{10}F_{10}$]$^{2-}$	0.40	n/a	n/a	0.05	n/a	n/a
[*closo*-$B_{10}Cl_{10}$]$^{2-}$	1.68	1.80	0.12	1.42	1.55	0.13
[*closo*-$B_{10}Br_{10}$]$^{2-}$	1.97	2.15	0.18	1.75	1.90	0.15
[*closo*-$B_{10}I_{10}$]$^{2-}$	2.17	2.50	0.33	2.03	2.15	0.12
[*closo*-$B_{10}At_{10}$]$^{2-}$	1.96	n/a	n/a	1.71	n/a	n/a
[*closo*-$B_{11}F_{11}$]$^{2-}$	0.43	n/a	n/a	0.02	n/a	n/a
[*closo*-$B_{11}Cl_{11}$]$^{2-}$	1.65	1.80	0.15	1.4	1.55	0.15
[*closo*-$B_{11}Br_{11}$]$^{2-}$	1.93	2.10	0.17	1.72	1.90	0.18
[*closo*-$B_{11}I_{11}$]$^{2-}$	2.15	2.40	0.25	2.01	2.15	0.14
[*closo*-$B_{11}At_{11}$]$^{2-}$	1.78	n/a	n/a	1.72	n/a	n/a
[*closo*-$B_{12}F_{12}$]$^{2-}$	1.80	1.90	0.10	1.41	1.7	0.29
[*closo*-$B_{12}Cl_{12}$]$^{2-}$	2.76	2.95	0.19	2.6	2.77	0.17
[*closo*-$B_{12}Br_{12}$]$^{2-}$	2.86	3.2	0.34	2.75	2.98	0.23
[*closo*-$B_{12}I_{12}$]$^{2-}$	2.36	2.8	0.44	2.34	2.75	0.41
[*closo*-$B_{12}At_{12}$]$^{2-}$	1.91	n/a	n/a	1.89	n/a	n/a

less electronically stable than the respective dodecaborate anions (n = 12). Recently, we have reported that the electronic stability of dodecaborate anions along the halogen series increases from F to Br but decreases from Br to I,[29] (see Figure 2). In contrast, the *closo*-borate anions with n = 10 and 11 exhibit a monotonic stabilization from X = Cl over Br to I by increments of roughly 0.3 eV. The different behavior of {*closo*-B_{10}} and {*closo*-B_{11}} MCAs when compared to the {*closo*-B_{12}} cages justified a closer comparative theoretical investigation of the electronic structure of these anions. Previous studies demonstrated that density functional theory (DFT) with the PBE0 functional provided an accurate description of the geometries of *closo*-borate anions.[30] The results in Table 1 show that PBE0 reproduces the experimental trends in the VDEs for all the investigated *closo*-borate anions quite well, albeit systematically underestimates the experimental values by 0.2 ± 0.1 eV for X = Cl, Br and 0.3 ± 0.1 eV for X = I. The spectral patterns and peak separations have inherent correlations with the molecular density of states (DOS). We found considerable disagreement between the observed spectral bands and the predicted DOS using the PBE0 functional (see SI2). In contrast, the DOS predicted by Hartree-Fock (plotted below the spectra in Figure 2) showed much better agreement with the experimental bands. In addition, we also present theoretical predictions for the VDEs, ADEs, and DOS of X = F, At and n = 10, 11, which are not yet experimentally available (see Table 1 and SI3). Neither the synthesis of [*closo*-$B_{10}F_{10}$]$^{2-}$ nor of [*closo*-$B_{11}F_{11}$]$^{2-}$ have been reported and these anions cannot be investigated experimentally. In the case of the decaboron cluster, only partial fluorination was experimentally achieved to yield [*closo*-$B_{10}H_{10-n}F_n$]$^{2-}$ (n = 1–4),[31] while in case of the undecaboron cage the anions [NC-*closo*-$B_{11}H_{10-n}F_n$]$^{2-}$ (n = 8–10) are the only fluorinated derivatives that are known so far.[32] The fluorinated boron clusters are of high interest as weakly coordinating anions[12] with potential applications for metal ion batteries[28c] and, in addition, *closo*-borates that carry fluorine or astatine atoms may be both of interest for diagnostic medical applications.[19b,33]

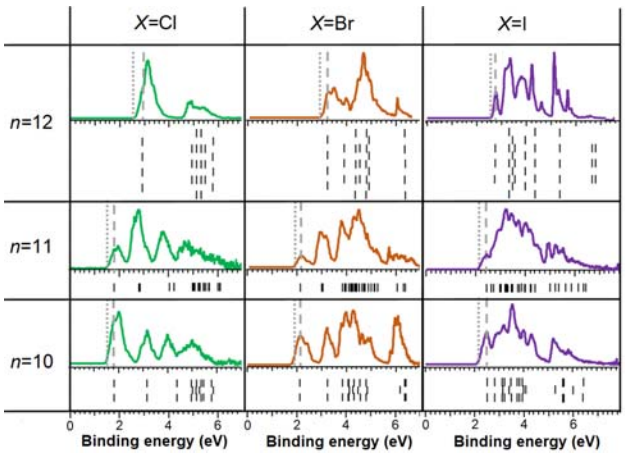

Figure 2 Comparison between the experimental PES spectra of *closo*-dodecaborate anions (n = 12, upper row) reported in Ref.[29] and the PES spectra (157 nm) of *closo*-undecaborate anions (n = 11, X = Cl–I, middle row) and *closo*-decaborate anions (n = 10, X = Cl–I, bottom row) obtained in this study. Dashed lines indicate VDEs and dotted lines ADEs. Black lines below the spectra denote the density of states (DOS) predicted by Hartree-Fock calculations. Note that the highest occupied molecular orbital (HOMO) energy was shifted to match the experimental VDE, see detailed explanations in SI1.

Our theoretical investigation suggested that the Highest Occupied Molecular Orbital (HOMO) of all fluorinated clusters consists predominantly of boron-centered orbitals. Going down the halogen series from F to At, an increased mixing of these boron-centered orbitals with halogen-centered orbitals takes place. This mixing is accompanied by a decrease in the energy of the boron-centered and concomitant increase in the energy of the halogen centered orbitals, see Figure 3. As a result, the boron-centered HOMO is more strongly stabilized with increase in the size of the halogen atom, which explains the increase in the electronic stability along the series of halogens. This finding is in agreement with the experimental and

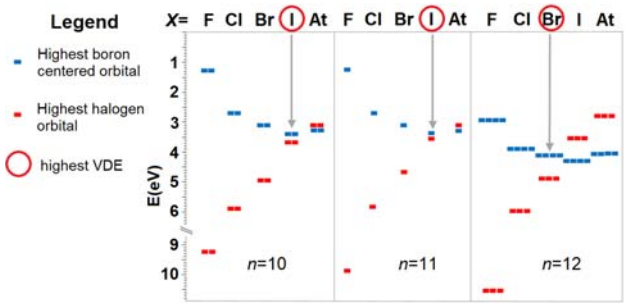

Figure 3 Simplified orbital diagrams showing the progression in orbital energy of the highest halogen- and boron-centered orbitals for *closo*-deca- (n = 10), *closo*-undeca- (n = 11), and *closo*-dodecaborate anions (n = 12) along the halogen series and the degree of degeneracy. Note that the so-called boron-centered orbitals consist of almost pure boron orbitals for X = F but become stabilized along the halogen series due to increased mixing with halogen-centered orbitals. Therefore, the HOMO is stabilized along the series although the halogens become less electronegative. A detailed diagram showing all orbitals up to a binding energy of 7 eV and their symmetry can be found in SI3 for n = 10, 11 and for n = 12 in the literature.[29]

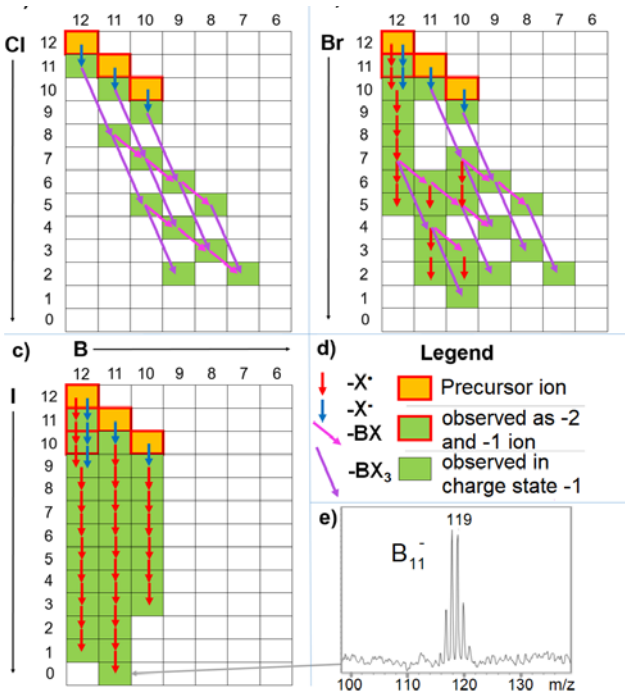

Figure 4 Diagrams summarizing the fragmentation pathways observed for [*closo*-B_nX_n]$^{2-}$ with n = 10–12 and X = Cl, Br, I in CID experiments (panels (a) - (c)). All molecular formula combinations of boron and halogen atoms, which have been observed, are shown. The legend in panel (d) explains the icons for the observed ions and neutral losses. Panel 4(e) shows the mass spectrum of the B_{11}^- ion, the product of the complete successive dehalogenation of the [*closo*-$B_{11}I_{11}$]$^{2-}$ ion by CID. CID of [$B_{12}F_{12}$]$^{2-}$ has been reported in ref. 34. We note that mass spectra may contain additional signals resulting from reactions of fragments with background gases like water as observed previously.[34]

calculated VDEs and ADEs listed in Table 1, with the exception of the [*closo*-$B_{12}I_{12}$]$^{2-}$ anion. The reason for this exception is that for this anion the iodine-centered orbitals are already higher in energy than the boron-centered orbitals, whereas for [*closo*-$B_{11}I_{11}$]$^{2-}$ and [*closo*-$B_{10}I_{10}$]$^{2-}$ the HOMOs are boron-centered orbitals. The respective point along the halogen series at which the halogen orbitals become higher in energy than the boron centered orbitals is found for the smaller clusters with n = 10 and 11 at iodine/astatine (see grey arrows in Figure 3), which makes the effect experimentally not observable as experiments with X = At are currently not feasible. Hence, for n = 12 the orbitals centered on the boron cage are very stable and the effect is found earlier along the halogen series (between bromine and iodine).

It is worth noting that considerable similarities of both the spectral band positions and spacings for the *closo*-borate anions with n = 10 and 11 and the same halogen substituent X are evident from the PES spectra (Figure 2) and the DOS in the orbital diagrams (SI3). In contrast, the corresponding spectra for the clusters with n = 12 are remarkably different. We conclude that from an electronic structure point of view, undecaborate anions (n = 11) are close relatives of decaborate anions (n = 10), but are less similar compared to the respective dodecaborate anions (n = 12).

A.2. Fragmentation pathways of [*closo*-B_nX_n]$^{2-}$: CID of dodecaborate anions (n = 12) has been previously reported.[34] Energetic collisions with an inert gas result in vibrational excitation of the ion followed by its fragmentation. The experimentally observed fragmentation pathways are summarized in Figure 4.

The first fragmentation reaction of the [*closo*-B_nX_n]$^{2-}$ ions occurs predominantly through the loss of a halide anion X^- (blue arrow), which is driven by charge separation. Radical halogen, $X^\bullet$, loss (red arrow) as a competing fragmentation channel was observed in small amounts for [*closo*-$B_{12}Br_{12}$]$^{2-}$ and is the dominant fragmentation channel for [*closo*-$B_{12}I_{12}$]$^{2-}$. The n = 10 and 11 species fragment only by halide ion loss. This may be attributed to the high thermodynamic stability of the doubly charged state of the dodecaborate anions. Subsequent fragmentation of the singly charged [*closo*-B_nX_{n-1}]$^-$ ions occurs through three different pathways: 1) loss of a BX_3 unit (purple arrow), 2) loss of a BX unit (pink arrow), and 3) loss of a halogen radical, $X^\bullet$ (red arrow). The competition between boron cage degradation (1 and 2) and radical halogen loss (3) was found to be strongly dependent on X. For example, the iodinated anions fragment almost exclusively by successive loss of iodine radicals (3). In contrast, chlorinated species show cage fragmentation (1 and 2) but no radical halogen loss (3). All three pathways are present for X = Br. This trend may be attributed to a decrease in stability of BX_3 formed in (1) and the decreasing boron–halogen bond strength with increasing halogen size. The observation of all three pathways for X = Br provides insights into the less pronounced influence of n on the observed fragmentation. Specifically, for n = 10 and 11 the brominated clusters follow mostly the boron cage degradation pathways (1 and 2), while for n = 12 a larger tendency for radical halogen loss (3) was observed. This is indicative for the higher structural stability of the B_{12} unit in comparison to the B_{10} and B_{11} ones.

The successive dehalogenation (with simultaneous preservation of the number of boron atoms) observed for all X = I *closo*-borate anions is an unusual dissociation pathway that has been examined earlier in detail both theoretically and experimentally only for n = 12.[35] It was found that the polyhedral boron unit undergoes considerable structural changes during the stripping of iodine because pure boron moieties are known to be quasi-planar.[36] Bare boron units have been previously investigated theoretically and experimentally due to their

exceptional bonding properties[36a,37] that became of interest, for example, in the context of molecular machines.[37c,37d] For n = 12, the formation of a naked B_{12} unit by de-iodination was not observed by mass spectrometry because, in the final step, $[B_{12}I]^-$ splits I^- (and not $I^\bullet$) due to the aromaticity of the neutral B_{12} unit, which is an energetically favorable product. In contrast to B_{12}, bare B_{11} clusters are aromatic as singly negatively charged ions.[36a] In agreement with this, $[B_{11}I]^-$ undergoes fragmentation to B_{11}^- as shown in Figure 4(c) and 4(e). The surprising observation of a bare boron unit generated through dissociation of iodinated *closo*-borate anions interconnects two very different fields of boron chemistry: polyhedral molecular borate anions that are stable in the condensed and the gas phase and naked boron clusters, being solely stable in the gas phase.

B. Interaction with cations in the gas phase

The interaction of *closo*-borate anions of the type $[closo\text{-}B_nX_n]^{2-}$ ($n \leq 12$, X = H, halogen) with cations has been studied in the condensed phase.[3-4,5b,38] In particular, perhalogenated 12-vertex anions $[closo\text{-}B_{12}X_{12}]^{2-}$ (X = F–Br)[10,30b] have been investigated in terms of their weakly coordinating properties. In the course of our study, we produced anionic ion pairs of the type $([closo\text{-}B_nX_n]+Bu_4N)^-$ (Bu_4N = tetrabutylammonium) in the gas phase with the aim to compare interactions of *closo*-borate anions with cations on a fundamental level without the influence of solvent shells and other interacting ions.

B.1. Electronic stabilization due to cation interaction with $[closo\text{-}B_nX_n]^{2-}$: The interaction of the doubly negatively charged *closo*-borate ions with a cation results in further stabilization of the orbitals of the borate ions. The comparison of the PES spectra of $([closo\text{-}B_nCl_n]+ Bu_4N)^-$ with those of $[closo\text{-}B_nCl_n]^{2-}$ (see SI5) shows that the Bu_4N cation induces a shift of all bands to higher binding energies but does not considerably influence the spectral pattern (band shape and relative signal separation), suggesting that the structure of the anions is not substantially altered upon complexation with cations. This is in agreement with previous investigations of *closo*-dodecaborates with transition metal cations via infrared spectroscopy investigations in the gas phase.[39] Note that PES experiments for X = Br and I were not possible with our instrument due to the high m/z ratio of these ion pairs. The stabilizing effect of cations on the electron binding energy of anions is strongly distance-dependent and it is therefore expected to decrease with increasing anion size. We observed an electronic stabilization of 2.5 eV for n = 10 and 11 but a significantly smaller effect of 2.3 eV for n = 12. A natural population analysis (see SI5) suggests that the negative charge is more localized in the 11-vertex anions, which possess a lower symmetry (Figure 1), whereas it is more uniformly distributed in the case of the more symmetric anions composed of 10 or 12 boron atoms. Therefore, the interplay between anion size and charge distribution may explain the obviously similar strong coordination of the Bu_4N cation for the 10- and 11-vertex anions: The larger ion size of $\{closo\text{-}B_{11}\}$ should result in a weaker coordination than for $\{closo\text{-}B_{10}\}$, while the more localized charge accounts for stronger Coulomb interactions. To confirm this assumption, we investigated the VDEs of $[closo\text{-}B_nCl_n]^{2-}$ with an ammonium ion at different coordination sites theoretically. Only the lowest-energy structure, in which the counter cation is coordinated to the surface spanned by the boron atoms 1, 2, 3, 5, and 6 (see Figure 1), resulted in a computed VDE that is very similar to the experimental value (see details in SI6). This indicates that the counter ion is predominantly located on this specific binding site, a fact implying that the fluctuation of the $\{closo\text{-}B_{11}\}$ cage known from the solution phase (*vide supra*) may be reduced in a gaseous, directly interacting ion pair. The length of the alkyl chain of the ammonium ion (methyl vs butyl) had only negligible influence on the electronic stabilization in our calculations, see SI6.

B.2. Ion pair fragmentation: We investigated fragmentation reactions of the precursor ions $([closo\text{-}B_nX_n]+ Bu_4N)^-$. Dissociation against Coulomb attraction is usually not observed in the gas phase. Instead, loss of neutral fragments is observed in CID spectra of the ion pairs. The observed fragments were divided into 3 different categories, as shown schematically in Figure 5(a). Since neutrals are not observed, the neutral components listed in the following equations may correspond to the sum of all neutral fragments. In particular, the fragments were formed via:

(i) **Anion decay:** The decay of the dianion in the ion pair is initiated by the electrophilic attack of the Bu_4N cation or a fragment of this cation that abstracts a negative substituent from the cluster resulting in a $[closo\text{-}B_nX_{n-1}]^-$ monoanion, which may subsequently generate secondary products:

$([closo\text{-}B_nX_n]+ Bu_4N)^- \rightarrow [closo\text{-}B_nX_{n-1}]^- + [XN(C_4H_9)_4]$

The secondary fragmentation of the $[closo\text{-}B_nX_{n-1}]^-$ anion is shown in Figure 4.

(ii) **Anion oxidation:** A redox reaction between the dianion and the Bu_4N cation occurs, leading to a singly charged radical anion:

$([closo\text{-}B_nX_n]+ Bu_4N)^- \rightarrow [closo\text{-}B_nX_n]^{-\bullet} + [N(C_4H_9)_4]^\bullet$,

Secondary fragmentation of $[closo\text{-}B_nX_n]^{-\bullet}$ occurs through the loss of $X^\bullet$ and formation of $[closo\text{-}B_nX_{n-1}]^-$.

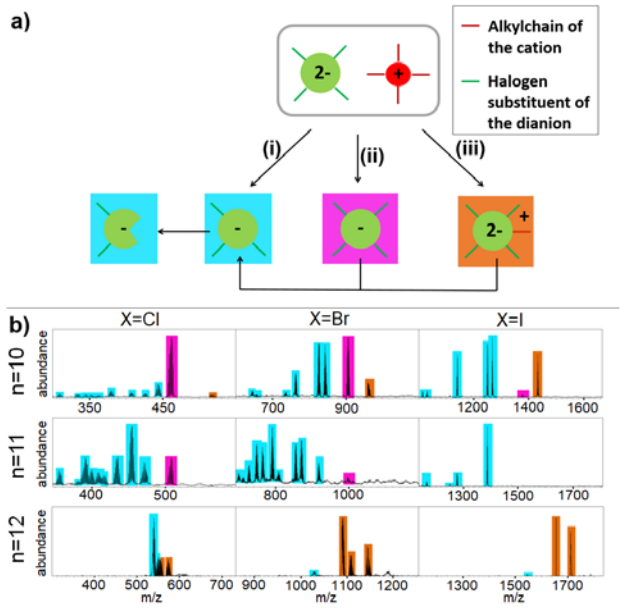

Figure 5 Fragmentation pathways of $([closo\text{-}B_nX_n]+ Bu_4N)^-$ after CID. (a) Scheme showing the different competing reaction pathways, (b) product ion spectra. Signals are marked with colors assigning them to one of the reactions shown in panel (a).

(iii) **Anion alkylation:** Instead of abstracting a negative substituent from the dianion, the cation dissociates into a neutral molecule and a butyl cation, which remains attached to the anion:

$([closo\text{-}B_nX_n]+ Bu_4N)^- \rightarrow [B_nX_n(C_4H_9)]^- + N(C_4H_9)_3$.

In the case of the 12-vertex clusters, secondary fragmentation of the butyl chain gives $[closo\text{-}B_nX_nH]^-$ (see SI7 for details), which undergo subsequent loss of H*X* resulting in $[closo\text{-}B_nX_{n-1}]^-$.

The product ion spectra of $([closo\text{-}B_nX_n]+ Bu_4N)^-$ shown in Figure 5(b) may be rationalized by the competition between the three fragmentation channels (i), (ii), and (iii). Pathway (ii) (electron transfer, purple highlights) is the dominant channel for *n* = 10 but less pronounced for *n* = 11 and absent for *n* = 12. This oxidation reaction of the anion is directly connected to the electronic stability investigated in Section A.1. The absence of this reaction for *n* = 12 is easily explained by the high electronic stability of dodecaborate anions. However, it is remarkable that the relative abundance of the $[closo\text{-}B_nX_n]^{\bullet-}$ fragment (purple) in CID spectra observed for *n* = 11 is much lower compared to *n* = 10, despite their very similar electronic stabilities. The higher relative intensity of signals associated with anion decay (channel (i), turquoise) for *n* = 11 indicates therefore a lower chemical stability of the dianion and its 11-vertex central boron unit compared to the respective 10-vertex analogues. This observation nicely reflects the lower chemical stability/higher reactivity of {*closo*-B_{11}} compared to {*closo*-B_{10}} and especially {*closo*-B_{12}} clusters known from the condensed phase (*vide infra*).[3-4,5b] Reaction products of type (iii) (orange) formed via alkylation of the *closo*-borate anion are dominant for *n* = 12. Dodecaborate anions are well-known for their high stability against electrophilic attack, which is necessary for abstraction of a negative substituent by a cation. In the condensed phase, these anions are resistant even against highly reactive alkyl cations,[10a] protons,[10d,40] and silylium ions.[10c] CID spectra of alkylated species shown in Figure 5(b) are consistent with this assertion. Decay of the anion by negative ligand abstraction is of low importance for *n* = 12 and the alkylated species $[B_nX_n(C_4H_9)]^-$ are observed. This reaction path (orange) is less pronounced for *n* = 10 and absent for *n* = 11. It is worth noting that products of anion decay (i) are more pronounced in the spectra for *X* = Cl, while products of the alkyl transfer reaction (iii) give almost the only observed signals in the case of *X* = Br, I for *n* = 12.

C. Condensed phase

After describing the electronic structure and reactivity of free gas phase boron cluster ions in Part A and the influence of a single counterion on these properties in Part B, this section augments the comparative study on $[closo\text{-}B_nX_n]^{2-}$ (*X* = Cl, Br, I; *n* = 10–12) to the condensed phase. The first part C.1 describes the electronic properties in the condensed phase by electrochemical measurements. In the second part C.2 selected aspects of the reactivity in the condensed phase are presented. These investigations allow to evaluate the meaning of intrinsic molecular properties determined in the gas phase for condensed phase applications.

C.1. Electrochemistry: A detailed, electrochemical study by cyclic voltammetry (CV) measurements for all clusters with *n* = 10, 11 and 12 in CH_3CN was undertaken for the first time to guarantee comparability of the measurements. So far, related studies have been performed only separately for the different cluster types using different conditions, e.g. different solvents, electrolytes, and reference electrodes (see Table S3–S5 in the SI9 for details). For example, previously reported CVs were recorded for solutions of $Na_2[closo\text{-}B_{12}X_{12}]$ (*X* = Cl, Br, I) in SO_2 and $Na_2[closo\text{-}B_{12}Cl_{12}]$ in CH_3CN.[16b] The data reported are in reasonable agreement to the ones found by us taking the different conditions into account. However, $[closo\text{-}B_{12}I_{12}]^{2-}$ is an exception. The first oxidation potential (E_{pa1}) for $Na_2[closo\text{-}B_{12}I_{12}]$ in SO_2 at –56 °C was reported as +2.1 V.[16b] A detailed electrochemical investigation of $[nBu_4N]_2[closo\text{-}B_{12}I_{12}]$ in acetonitrile at room temperature gave a much lower E_{pa1} of +1.41 V (Figure 6 and Figure S9 in the SI9). This comparably large difference proves the necessity of performing CV studies using the same conditions to enable a valid comparison. The redox chemistry of $[Et_3BzN]_2[closo\text{-}B_{11}X_{11}]$ (*X* = Cl, Br, I)[41] and of salts of the ions $[closo\text{-}B_{10}X_{10}]^{2-}$ (*X* = Cl, Br, I)[42] was

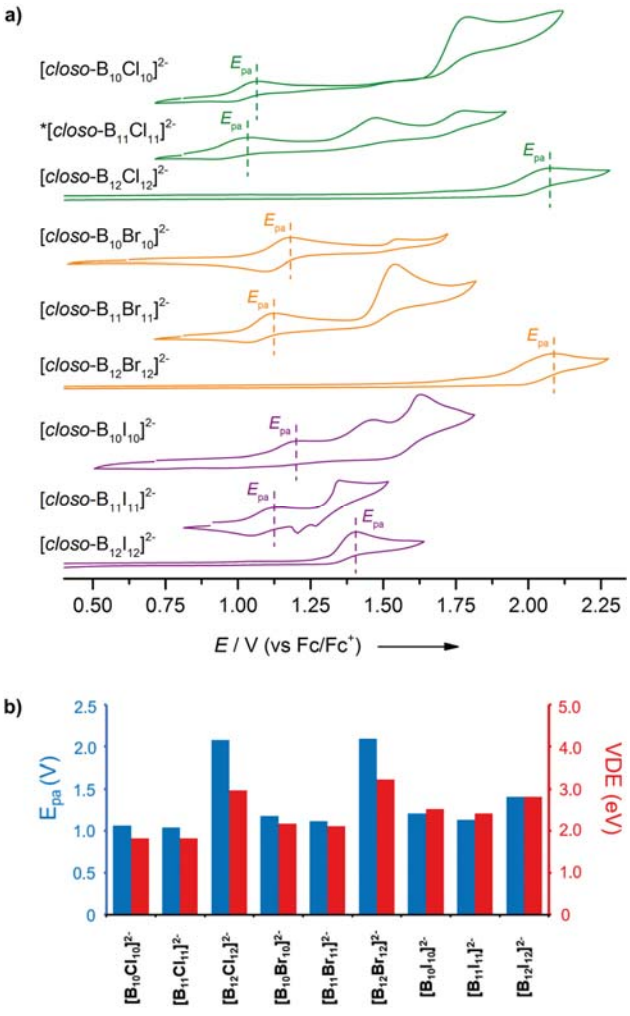

Figure 6 a) Cyclic voltammograms of $[nBu_4N]_2[closo\text{-}B_nX_n]$ (*X* = Cl, Br, I; *n* = 10–12) in CH_3CN (top, $c = 1{\cdot}10^{-3}$ mol L^{-1}; scan rate $v = 100$ mV s^{-1}, glassy-carbon working electrode, Pt counter electrode, reference electrode 0.01 mol L^{-1} $AgNO_3$ and 0.1 mol L^{-1} $[nBu_4N][PF_6]$; $*[nBu_4N]_2[closo\text{-}B_{11}Cl_{11}]$ contains 33% of $[nBu_4N]_2[closo\text{-}B_{10}Cl_{10}]$, see Table S6 in SI9 and Figures S8–S10 for CVs with extended ranges). Dashed lines mark the first oxidation potential b) Comparison of the peak oxidation potentials (E_{pa}) in solution and vertical detachment energies (VDE) of the dianions $[closo\text{-}B_nX_n]^{2-}$ in the gas phase, see text for details.

studied before, as well. However, the data are not complete as exemplified by the ones of $[Et_3BzN]_2[closo\text{-}B_{11}X_{11}]$ (X = Cl, Br, I)[41] in Table S3 in the SI9.

The CVs of the perhalogenated {*closo*-B_n} (n = 10–12) clusters measured in our comparative investigation are depicted in Figure 6a. The first oxidation potentials for {*closo*-B_{10}} and {*closo*-B_{11}} clusters are very similar with slightly lower values for the 11-vertex derivatives in all cases, while considerably higher potentials are necessary to oxidize the {*closo*-B_{12}} clusters. As demonstrated in Figure 6b, the relative trends observed for the electron detachment probed by gas-phase PES for the free anions and their oxidation in solution by electrochemical measurements are very similar. Although the absolute values for the electron detachment in the gas phase and the measured oxidation potentials during CV experiments cannot be directly compared to each other, a comparison of the relative values may provide some insights about the electronic stabilization of the different ions in condensed phase. The y-axes in Figure 6(b) are scaled so that the oxidation peak potential in acetonitrile (E_{pa}, red) and the VDE value (blue) for $[closo\text{-}B_{12}I_{12}]^{2-}$ are displayed at the same height. Therefore, if for another ion the blue bar in Figure 6b is larger than the red bar, this may be associated with a stronger electronic stabilization in solution than the one for $[closo\text{-}B_{12}I_{12}]^{2-}$, while a larger red bar may be associated with a weaker stabilization. So, the bar diagram indicates a gain in electronic stabilization in solution with decreasing size of the halogen X. This effect may be traced back to a smaller ion-size and an increased partial charge on the substituent shell, which results in an increase in the interaction with solvent molecules and counter ions. The results of theoretical investigations on ion-acetonitrile interaction are provided in SI8. However, the trend dependent on n is opposite to the increase in the ion size. A remarkably larger electronic stabilization for the 12-vertex clusters in solution is found relative to the clusters with n = 10 and 11 as inferred from the data. Possible explanations for this effect may be due to an increased number and a different orientation of solvent molecules in the first solvation shell of the n = 12. However, Born-Oppenheimer Molecular Dynamics (BOMD) simulations (see SI10) do not indicate considerable differences in the solvent shells of the exemplary studies {*closo*-B_{10}} and {*closo*-B_{12}} clusters for X = Cl. This implies that very complex models may be necessary to describe the condensed phase effects on the electronic stabilization adequately.

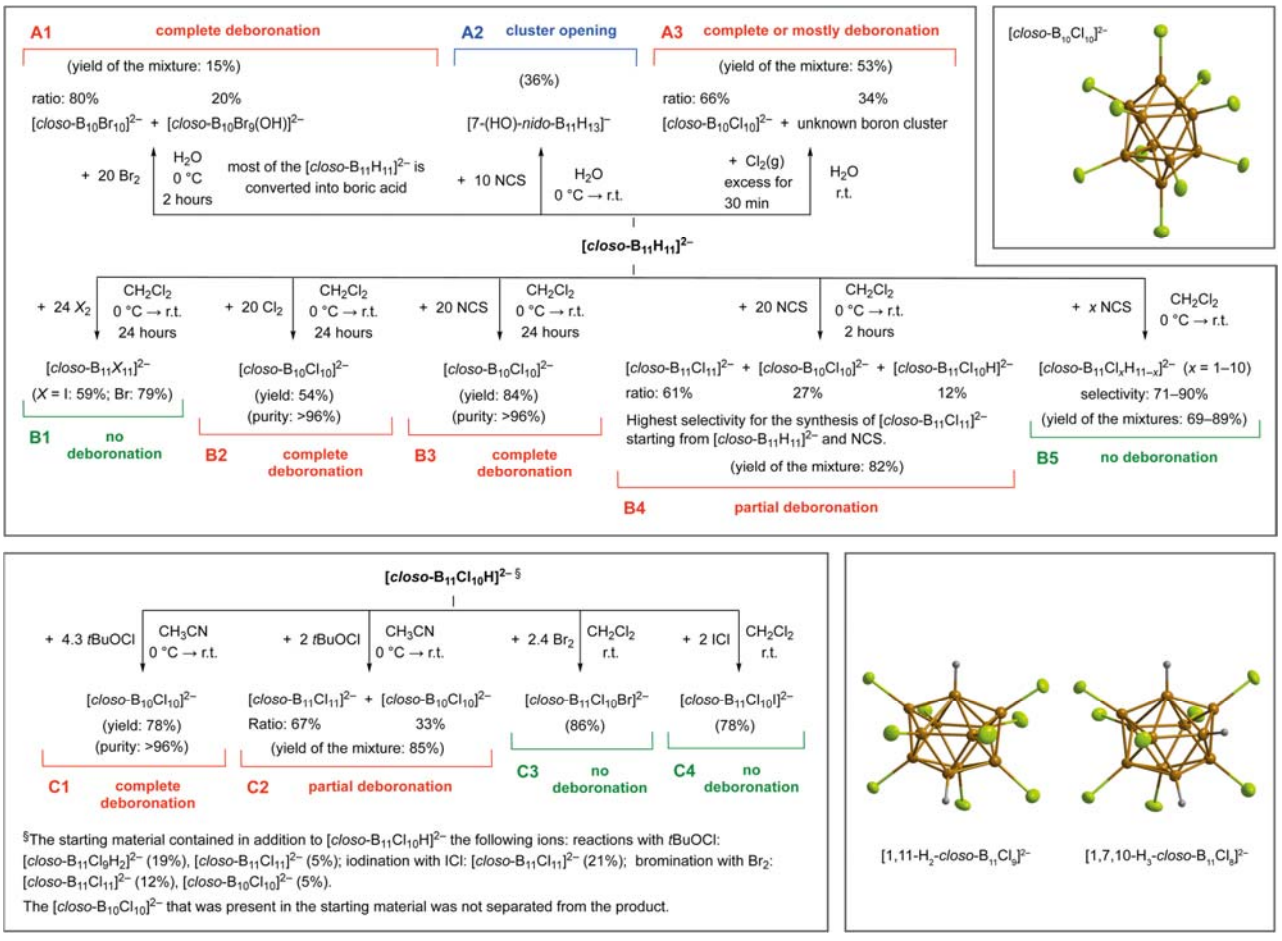

Scheme 1 Synthesis of $[nBu_4N]^+$ salts of $[closo\text{-}B_{11}Cl_{11}]^{2-}$ and $[closo\text{-}B_{10}Cl_{10}]^{2-}$ and successive chlorination of $[nBu_4N]_2[closo\text{-}B_{11}H_{11}]$. Structures of the dianions $[1,11\text{-}H_2\text{-}closo\text{-}B_{11}Cl_9]^{2-}$ and $[1,7,10\text{-}H_3\text{-}closo\text{-}B_{11}Cl_8]^{2-}$ as well as $[closo\text{-}B_{10}Cl_{10}]^{2-}$ in the crystals of the salts $[nBu_4N]_2[closo\text{-}B_{11}Cl_xH_{11-x}]\cdot(CH_3)_2CO$ (x = 8 (50%); 9 (50%)) and $[nBu_4N]_2[closo\text{-}B_{10}Cl_{10}]$, respectively. Ellipsoids are set at 20% probability, except for H atoms that are depicted with arbitrary radii. Details of the structure refinements can be found in the SI. [Purities given are based on ^{11}B NMR spectra.]

C.2. Condensed phase reactivity: In the condensed phase, the chemistry of the {*closo*-B_{12}} cluster is the most detailed studied among all dianionic {*closo*-B_n} cages,[3] followed by the one of the {*closo*-B_{10}} cage.[4] Reactions of {*closo*-B_{11}} derivatives are far less explored. Most likely, this is due to (*i*) the much higher reactivity of the {*closo*-B_{11}} cage and (*ii*) the limited availability of its derivatives.[5b] A few years ago, a convenient and efficient synthesis of [*closo*-$B_{11}H_{11}]^{2-}$ salts was published providing an easy, alternate access to this class of compounds and facilitating systematic studies of their properties.[43] This solution-based method complements a previous high-yield solid-state pyrolysis synthesis.[44]. Already in their pioneering work, Klanberg and Muetterties described the deboronation of the {*closo*-B_{11}} cage to yield {*closo*-B_{10}} clusters establishing the comparably high reactivity of these ions. They reported the deboronation of the [*closo*-$B_{11}H_{11}]^{2-}$ ion in the course of halogenation reactions with Br_2 and *N*-chlorosuccinimide (NCS) in acidic media to give primarily [*closo*-$B_{10}Br_{10}]^{2-}$ and [*closo*-$B_{10}Cl_8H_2]^{2-}$, respectively.[5a] Under basic aqueous conditions bromination did not proceed via deboronation as evident from analytic data, which were indicative for the formation of [*closo*-$B_{11}Br_9H_2]^{2-}$.[5a] Later, Tolpin and Lipscomb reported the synthesis of $[Me_4N]_2$[*closo*-$B_{11}Br_4H_7$] from [*closo*-$B_{11}H_{11}]^{2-}$ and Br_2 in caustic soda but multiple recrystallization was necessary and no yield was given.[6a] For {*closo*-B_{12}} and {*closo*-B_{10}} clusters related deboronation reactions are unknown,[3-4] underlining the lower stability of the 11-vertex *closo*-cluster along the dimension *n* in the {*closo*-B_n} series. We reinvestigated the halogenation/deboronation reactions of the {*closo*-B_{11}} cage (Scheme 1)[5a,41] as a model for a comparative picture of the reactivity along both dimensions *n* and *X* of [*closo*-$B_nX_n]^{2-}$ in the condensed phase (*vide supra*).

We confirmed the formation of [*closo*-$B_{10}Br_{10}]^{2-}$ but with [*closo*-$B_{10}Br_9(OH)]^{2-}$ as a side product upon bromination of [*closo*-$B_{11}H_{11}]^{2-}$ in water using modern analytical techniques (Scheme 1, **A1**). However, the yield is low (<15%) and boronic acid is the main product. Formation of [*closo*-$B_{11}Br_9H_2]^{2-}$ was not confirmed, also not under basic conditions. In fact, we did not observe any pH dependency of this bromination reaction in water (for more details see SI11). Deboronation of the {*closo*-B_{11}} cage during chlorination with NCS in water was not reproduced in our hands,[5a] but the known anion [7-(HO)-*nido*-$B_{11}H_{13}]^-$[45] was isolated instead (Scheme 1, **A2**). In contrast, chlorine and [*closo*-$B_{11}H_{11}]^{2-}$ gave [*closo*-$B_{10}Cl_{10}]^{2-}$ together with an unknown boron cluster species in a 2:1 mixture in a combined yield of approximately 53% (Scheme 1, **A3**). These results substantiate the significantly higher reactivity of the 11-vertex cluster since halogenation reactions of [*closo*-$B_{12}H_{12}]^{2-}$ [30a,42c,46] and [*closo*-$B_{10}H_{10}]^{2-}$ [42c] in aqueous media or alcohols are well-known to give [*closo*-$B_nX_n]^{2-}$ (*X* = Cl, Br; *n* = 10, 12), respectively (for details see SI11).[3-4]

Halogenation of the [*closo*-$B_{11}H_{11}]^{2-}$ ion in dichloromethane with elemental Cl_2, Br_2 and I_2 was studied to evaluate the influence of *X* on the reactivity, especially, since no definite trend was found for previously investigated reactions in water. In case of *X* = Br and I, the perhalogenated anions [*closo*-$B_{11}X_{11}]^{2-}$ were obtained in high purity with yields of 79 and 59%, respectively (Scheme 1, **B1**). Similar yields were reported earlier for the benzyltriethylammonium salts (Br: 84%, I: 33%).[41] In contrast, the reaction with Cl_2 resulted in [*closo*-$B_{10}Cl_{10}]^{2-}$ in 54% yield (Scheme 1, **B2**). To gain a deeper insight into the deboronation, we explored chlorination under different conditions. NCS and *tert*-butyl hypochlorite (*t*BuOCl) were both found to react under deboronation in CH_2Cl_2 or CH_3CN, also, and [*closo*-$B_{10}Cl_{10}]^{2-}$ was obtained in up to 84% yield from [*closo*-$B_{11}H_{11}]^{2-}$ or [*closo*-$B_{11}Cl_{10}H]^{2-}$ (Scheme 1, **B3** and **C1**). BCl_3 is the byproduct of this deboronation as evident from ^{11}B NMR spectra. Milder reaction conditions enabled the synthesis of [*closo*-$B_{11}Cl_{11}]^{2-}$ but the product was always contaminated with [*closo*-$B_{10}Cl_{10}]^{2-}$ (Scheme 1, **B4** and **C2**). Surprisingly, [*closo*-$B_{11}Cl_{10}H]^{2-}$ and all other partially chlorinated 11-vertex clusters [*closo*-$B_{11}Cl_xH_{11-x}]^{2-}$ (*x* = 1–9) were obtained by chlorination of [*closo*-$B_{11}H_{11}]^{2-}$ with NCS without any degradation to give 10-vertex clusters (Scheme 1, **B5**, detailed information and ^{11}B NMR spectra are collected in SI11). The ions [*closo*-$B_{11}Cl_9H_2]^{2-}$ and [*closo*-$B_{11}Cl_8H_3]^{2-}$ are the first partially halogenated {*closo*-B_{11}} clusters that were characterized by X-ray diffraction (Scheme 1) besides [NC-*closo*-$B_{11}F_{10}]^{2-}$.[32] Interestingly, bromination and iodination of [*closo*-$B_{11}Cl_{10}H]^{2-}$ gave [*closo*-$B_{11}Cl_{10}X]^{2-}$ (*X* = Br, I) in good yields without any deboronation products (Scheme 1, **C3** and **C4**; the iodination of [*closo*-$B_{11}Cl_{10}H]^{2-}$ was reported, earlier[41]). These findings contrast the chlorination of [*closo*-$B_{11}Cl_{10}H]^{2-}$ that always – independent on the conditions and the chlorination reagent used – yielded [*closo*-$B_{10}Cl_{10}]^{2-}$ as main or side product (Scheme 1, **C1** and **C2**),

The chlorination reactions conducted show that [*closo*-$B_{11}Cl_{11}]^{2-}$ is converted with Cl_2, *t*BuOCl or NCS into [*closo*-$B_{10}Cl_{10}]^{2-}$. Hence, deboronation occurs either during the last chlorination step of [*closo*-$B_{11}Cl_{10}H]^{2-}$ or thereafter from [*closo*-$B_{11}Cl_{11}]^{2-}$. In contrast, treatment of the perbrominated ion [*closo*-$B_{11}Br_{11}]^{2-}$ with elemental Cl_2 did not result in any deboronation.

These observations on condensed phase reactivities discussed, so far, prove the strong influence of *X* = Cl, Br, I on the reactivity and stability of {*closo*-B_n} (*n* = 10–12). This is further supported by a literature survey on fluorinated {*closo*-B_n} cages. [*closo*-$B_{12}F_{12}]^{2-}$ [10b,47] and related anions, e.g. [1-(H_3N)-*closo*-$B_{12}F_{11}]^-$,[11a,48] are accessible by fluorination with F_2. Partially fluorinated {*closo*-B_{12}} clusters have been obtained, as well,[15b,47b] e.g. by treatment of [*closo*-$B_{12}H_{12}]^{2-}$ with anhydrous HF.[49] In contrast, (i) the cages [*closo*-$B_nH_n]^{2-}$ (*n* = 10, 11) are disrupted in anhydrous HF,[31,50] (ii) fluorination of [*closo*-$B_{10}H_{10}]^{2-}$ gave partially fluorinated derivatives [*closo*-$B_{10}F_xH_{10-x}]^{2-}$ (*x* = 1–5), only,[31,51] and (iii) fluorination of [*closo*-$B_{11}H_{11}]^{2-}$ remained unsuccessful, so far.[50] Furthermore, highly fluorinated {*closo*-B_{12}} derivatives are highly stable,[10b,11a,47-48] whereas [NC-*closo*-$B_{11}F_{10}]^{2-}$ is much more reactive.[32,52]

The halogenation reactions of {*closo*-B_n} clusters (*n* = 10–12) reported herein and described in the literature establish a distinct picture of the structural stability/reactivity of [*closo*-$B_nX_n]^{2-}$ (*X* = Cl, Br, I, F; *n* = 10–12). Significant differences along the parameters cluster size *n* and halogen *X* are present in the condensed phase similar to the gas phase (vide supra). In addition, we introduce convenient, high-yield syntheses for [*closo*-$B_{10}Cl_{10}]^{2-}$ salts based on chlorination of K_2[*closo*-$B_{11}H_{11}$], which is readily available.[43-44]

Discussion

The electronic properties and reactivities of *closo*-borate anions [*closo*-$B_nX_n]^{2-}$ (*X* = halogen) have been compared following both

parameters cluster size (n = 10–12) and halogen substituent (X = Cl, Br, I) with the aim to bridge the gap between gas and condensed phase properties by investigating isolated anions, gaseous ion pairs, and salts in solution.

Electronic properties: According to our study on the electronic stability and structure of all anions [*closo*-B_nX_n]$^{2-}$ (n = 10–12, X = Cl–I) by photoelectron spectroscopy (PES) in the gas phase, {*closo*-B_{11}} clusters have very similar electronic properties compared to their {*closo*-B_{10}} analogs. {*closo*-B_{12}} clusters were found to be considerably more stable. Stabilization due to interactions with a single tetraalkylammonium cation in the gas phase was again found to be similar for {*closo*-B_{10}} and {*closo*-B_{11}} clusters despite their different cluster size. A specific coordination site for the ammonium cation to the comparably low-symmetric {*closo*-B_{11}} cluster is the main reason for this similarity. Cyclic voltammetry (CV) measurements show that the aforementioned trend in intrinsic molecular ion properties is very close to the trend of electronic properties in the condensed phase. The differences found for the gas phase and condensed phase data, in principle, allow a qualitative evaluation of the influence of the solvent and/or intermolecular interactions on the electronic properties, which may be an important topic of further studies.

Reactivity/Stability: The fragmentation behavior of the isolated anions [*closo*-B_nX_n]$^{2-}$ in the gas phase by mass spectrometry was found to be largely determined by the substituent X. Small halogens increase the tendency for boron unit fragmentation (through loss of BX_3 and BX units). For X = I, stripping of halogen substituents without boron unit fragmentation is favored and the bare B_{11}^- cluster was generated by stepwise removal of iodine from [*closo*-$B_{11}I_{11}$]$^{2-}$.

Pronounced differences in the molecular stability dependent on n were found upon fragmentation of the *closo*-borates with a single counterion in the gas phase. {*closo*-B_{12}}, followed by the {*closo*-B_{10}} cluster, are highly stable and stabilize reactive fragments of the countercation, while, in comparison, {*closo*-B_{11}} clusters exhibit anion decay and no stabilization of counter ion fragments.

In the condensed phase, the same reactivity trend as in the gas phase was evident for the [*closo*-B_nX_n]$^{2-}$ series. The {*closo*-B_{11}} cluster is by far the most reactive {*closo*-B_n} cage with n = 10–12 as shown herein and documented in the literature.[3-4,5b] Importantly, our comparison with intrinsic electronic properties proof that this is not due to an inherent electronic instability of the {*closo*-B_{11}} derivatives but a consequence of the specific properties of the cluster geometry, especially the B1 atom that has an inner-cluster connectivity of 6 (Figure 1).[5b,5c,32] In addition, the {*closo*-B_{11}} cage is fluxional in solution whereas the 10- and 12-vertex *closo*-clusters are rigid. The fluxional behavior is also related to the unusual bonding situation of the 11-vertex *closo*-boron cluster. We could further show that the increased tendency for cluster degradation with smaller halogens found for isolated gas-phase ions is also reflected in the condensed-phase reactivity. The [*closo*-$B_{10}Cl_{10}$]$^{2-}$ ion is selectively formed by chlorination starting from readily available salts of [*closo*-$B_{11}H_{11}$]$^{2-}$ via [*closo*-$B_{11}Cl_{10}H$]$^{2-}$/[*closo*-$B_{11}Cl_{11}$]$^{2-}$ as intermediates, whereas the boron cage structure is stable in bromination and iodination reactions under non-aqueous conditions. It is interesting to note that the product of the deboronation reaction BCl_3 investigated here is one of the dominant neutral losses also observed in CID experiments. Although reactions observed by CID experiments may differ *per se* from reactions occurring in the condensed phase, our study exemplifies that they may allow to understand and maybe predict differences in condensed phase chemical synthesis.

Conclusions

Perhalogenated *closo*-dodecaborate anions ([*closo*-$B_{12}X_{12}$]$^{2-}$) are notorious for their structural and electronic stability and chemical inertness, especially their resistance against electrophilic attack. The comparative study on the molecular level in the gas phase and in solution has evidenced that [*closo*-$B_{10}X_{10}$]$^{2-}$ anions exhibit similar, only slightly reduced chemical inertness and stability. It is obvious that the related [*closo*-$B_{11}X_{11}$]$^{2-}$ anions may not be used as weakly coordinating anions (WCA) because of their higher structural instability in comparison to their smaller and bigger neighbors with n = 10 and 12, respectively. However, the enhanced reactivity opens interesting possibilities for the functionalization and transformation of {*closo*-B_{11}} derivatives, as demonstrated recently.[5c] The fundamental, systematic evaluation and comparison of the electronic and chemical properties of 10-, 11- and 12-vertex *closo*-borate anions, provided with this study, can serve as reference for future developments in the field of *closo*-borate chemistry in the gas and condensed phase alike, because a rational design of *closo*-borates with specific properties becomes possible. Especially, this study shows that a sound knowledge of the gas phase properties of boron clusters can help synthetic chemists to understand and potentially to plan reactions in solution. A first example is the new and convenient synthesis for salts of the [*closo*-$B_{10}Cl_{10}$]$^{2-}$ ion introduced here, which makes them more easily available. This may stimulate its application especially in materials science and medicine.

Experimental

Photoelectron Spectroscopy

Photoelectron Spectroscopy (PES) experiments were performed with an apparatus consisting of an electrospray ionization source (ESI), a temperature-controlled cryogenic ion trap, and a magnetic-bottle time-of-flight (TOF) photoelectron spectrometer, as described elsewhere.[53] Acetonitrile solutions of *closo*-borate salts (0.1 mM) were used for electrospray. The ions generated by ESI were guided by quadrupole ion guides into the ion trap, where they were accumulated and cooled for 20-100 ms by collisions with a cold buffer gas (20% H_2 balanced in helium) at 20 K, before being transferred into the extraction zone of a TOF mass spectrometer. The cooling of the anions to 20 K improved spectral energy resolution and eliminated the possibility of the appearance of peaks in the PE spectra, due to hot bands. The anions were mass selected and decelerated prior to photodetachment with 157 nm photons (7.866 eV) from an F_2 excimer laser. The laser was operated at a 20 Hz repetition rate, with the ion beam off at alternating laser shots, affording shot-to-shot background subtraction. Photoelectrons were collected with ~100% efficiency using a magnetic bottle and analyzed in a 5.2 m long electron flight tube. The recorded TOF photoelectron spectrum was converted into an electron kinetic

energy spectrum by calibration with the known photoelectron spectra of I^- [54] and $[OsCl_6]^{2-}$.[55] The electron binding energy (EBE) was obtained by subtracting the electron kinetic energy from the energy of the detaching photons. The energy resolution was about 2%, i.e., ~20 meV for 1 eV kinetic energy electrons. Details about interpretation of PES spectra can be found in SI1.

Collision induced dissociation

Mass spectrometry experiments were performed on a Bruker HCT Ion Trap (Billerica, MA) or a Bruker Esquire LC Ion Trap (Bremen). Ions were dissolved in CH_3CN with concentrations of 10^{-6}–10^{-7} mol L^{-1} and injected via a syringe pump. An electrospray voltage of 3500–4000 V was applied and 300 °C nitrogen was used as dry gas. Collision-induced dissociation (CID) was induced in the nozzle-skimmer region (sCID) as well as in the ion traps. Ions were excited by collisions with a background gas (N_2, He) to higher vibrational modes until they fragmented. For sCID, the ions were accelerated using an adjustable potential gradient in the first pumping stage of the mass spectrometer's differential pumping system, i.e. at pressures of about 2.5 mbar. In the ion trap, ions with a defined m/z-value were isolated and activated by applying an adjustable ac voltage to the ion trap end caps. Ion trap CID experiments generate reaction products of the isolated and activated ions.

Cyclic voltammetry

Cyclic voltammetry experiments were performed with a Metrohm PGSTAT30 potentiostat. A standard three-electrode cell configuration was employed with a glassy carbon working electrode sealed in glass (external diameter Ø = 6 mm; internal diameter Ø = 3 mm: active surface area: 7.07 mm^2), a Pt-wire counter electrode (Ø = 3 mm; length: 5 cm), and an $Ag/AgNO_3$ reference electrode (0.01 mol L^{-1} $AgNO_3$ in acetonitrile that contained 0.1 mol L^{-1} [*n*Bu_4N][PF_6]) separated by a Vycor tip. Cyclic voltammograms were measured for solutions of [*n*Bu_4N]$_2$[*closo*-$B_{10}X_{10}$], [*n*Bu_4N]$_2$[*closo*-$B_{11}X_{11}$], and [*n*Bu_4N]$_2$[*closo*-$B_{12}X_{12}$] (*X* = Cl, Br, I), in anhydrous acetonitrile ($1\cdot10^{-3}$ mol L^{-1}). Data analysis was carried out with the Nova 1.10 and Nova 1.11 software suite.

Chemical synthesis

Reactions involving air-sensitive compounds were performed either in round bottom flasks or in glass tubes equipped with valves with PTFE stems (Rettberg, Göttingen and Young, London) under argon using standard Schlenk line techniques.

[*n*Bu_4N]$_2$[*closo*-$B_{10}Cl_{10}$] from [*n*Bu_4N]$_2$[*closo*-$B_{11}H_{11}$] and NCS. A CH_2Cl_2 (50 mL) solution of [*n*Bu_4N]$_2$[*closo*-$B_{11}H_{11}$] (0.50 g, 0.81 mmol) was treated with NCS (2.17 g, 10.26 mmol). After 1 d at r.t., a saturated aqueous solution of Na_2SO_3 (50 mL) was added. The organic phase was separated, and the aqueous layer was extracted with CH_2Cl_2 (3 x 50 mL). The combined organic phases were dried with $MgSO_4$. The solids were filtered off and all volatiles were removed using a rotary evaporator. Yield: 0.64 g (0.68 mmol, 84%; purity >96% [The salt contained <4% of [*n*Bu_4N]$_2$[*closo*-$B_{11}Cl_{11}$] as assessed by ^{11}B NMR spectroscopy]). ^1H NMR (500.13 MHz, CD_3CN): δ = 3.16 (m, 8H, CH_2), 1.67 (m, 8H, CH_2), 1.41 (m, 8H, CH_2), 1.02 (t, 12H, $^3J(^1H,^1H)$ = 7.3 Hz, CH_3). ^{11}B NMR (160.46 MHz, CD_3CN): δ = –3.3 (s, 2B, B1+12), –10.5 (s, 10B, B2–11) ppm. MALDI-MS *m/z* (isotopic abundance >45) cald. for [*closo*-$B_{10}Cl10]^{\bullet-}$: 459(48), 460(70), 461(89), 462 (100), 463 (100), 464(91), 465(74), 466(57); found: 459(51), 460(79), 461(93), 462(100), 463(99), 464(90), 465(74), 466(54).

[*n*Bu_4N]$_2$[*closo*-$B_{10}Cl_{10}$] from [*n*Bu_4N]$_2$[*closo*-$B_{11}H_{11}$] and Cl_2. An excess of chlorine was passed through a solution of [*n*Bu_4N]$_2$[*closo*-$B_{11}H_{11}$] (0.50 g, 0.81 mmol) in CH_2Cl_2 (50 mL) for 30 min. After stirring at r.t. for 1 d, a saturated aqueous solution of Na_2SO_3 (50 mL) was added. The organic layer was separated, and the aqueous layer was extracted with dichloromethane (3 x 50 mL). The combined organic phases were dried with $MgSO_4$. The solids were filtered off and the solvent was removed using a rotary evaporator. Yield: 0.42 g (0.44 mmol, 54%; purity >96% [The salt contained <4% of [*n*Bu_4N]$_2$[*closo*-$B_{11}Cl_{11}$] as assessed by ^{11}B NMR spectroscopy]).

[*n*Bu_4N]$_2$[*closo*-$B_{10}Cl_{10}$] from [*n*Bu_4N]$_2$[*closo*-$B_{11}Cl_{10}H$] and *t*BuOCl. *tert*-Butyl hypochlorite (0.16 mL, 0.15 g, 1.36 mmol) was added to a solution of [*n*Bu_4N]$_2$[*closo*-$B_{11}Cl_{10}H$] (0.30 g, 0.32 mmol) in CH_3CN (14 mL) in the dark at 0 °C. The solution was stirred at 0 °C for 8.5 h followed by stirring for 5 d at r.t. The solvent was removed under reduced pressure and the solid residue was dissolved in acetone (2 mL). Addition of water gave a precipitate that was isolated by filtration and subsequently dried in a vacuum. Yield: 0.25 g (0.26 mmol, 81%; purity >96% [The salt contained <4% of [*n*Bu_4N]$_2$-[*closo*-$B_{11}Cl_{11}$] as assessed by ^{11}B NMR spectroscopy]). Elemental analysis: calcd. (%) for $C_{32}H_{72}B_{10}Cl_{10}N_2$, C 40.56, H 7.66, N 2.96; found, C 40.68, H 7.51, N 3.02.

Further synthetic details can be found in SI11.

Theoretical investigations

The Vertical Detachment Energies (VDEs) were theoretically determined as energy differences between the singly charged anions and corresponding dianions (or neutrals and corresponding singly charged anions), both at the dianion's (anion's) optimized geometry. ADEs were determined as the energy difference between the geometrically optimized singly charged anions and corresponding dianions (or geometrically optimized neutrals and corresponding singly charged anions). All calculations were done using the NWChem software.[56] Geometry optimizations and electronic structure calculations were done with the DFT method PBE0[57] using the aug-cc-pVTZ basis set[58] or the def2-tzvppd basis set.[59] Dispersion correction[60] was applied if non-covalent interactions were investigated. Details of molecular dynamics simulations are described in the supporting information.

Acknowledgements

J.W. (recipient), J.L. and S.S.X. (hosts) acknowledge a Feodor Lynen Fellowship of the Alexander von Humboldt Foundation. M.F. is grateful to the Deutsche Forschungsgemeinschaft (DFG) for financial support (FI 1628/2-2). J.W. and J.L. acknowledge support by BES Separations and Analysis Program at PNNL. X.B.W. and S.S.X. acknowledge support from the U.S. Department of Energy, Office of Science, Office of Basic Energy Sciences, Division of Chemical Sciences, Geosciences and Biosciences at Pacific Northwest National Laboratory. Battelle operates the Pacific Northwest National Laboratory for the U.S. Department of Energy. This research used computer resources provided by EMSL, a DOE Office of Science User Facility sponsored by the Office of Biological and Environmental

Research and located at Pacific Northwest National Laboratory, PNNL Institutional Computing (PIC), and by the National Energy Research Scientific Computing Center, which is supported by the Office of Science of the U.S. Department of Energy under Contract No. DE-AC02-05CH11231. A portion of this research (E.A., E.B. and X.B.W.) was performed in EMSL.

Notes and references

1 A. Stock, *The Hydrides of Boron and Silicon (The George Fisher Baker Non-Resident Lectureship in Chemistry at Cornell University)*, Cornell University Press, Ithaca, New York, 1933.

2 W. N. Lipscomb, *Science*, 1977, **196**, 1047–1055.

3 I. B. Sivaev, V. I. Bregadze, S. Sjöberg, *Collect. Czech. Chem. Commun.*, 2002, **67**, 679–727.

4 I. B. Sivaev, A. V. Prikaznov, D. Naoufal, *Collect. Czech. Chem. Commun.*, 2010, **75**, 1149–1199.

5 (a) E. L. Klanberg, E. L. Muetterties, *Inorg. Chem.*, 1966, **5**, 1955–1960; (b) O. Volkov, P. Paetzold, *J. Organomet. Chem.*, 2003, **680**, 301–311; (c) S. Z. Konieczka, F. Schlüter, C. Sindorf, C. Kerpen, E. Bernhardt, M. Finze, *Chem. Eur. J.*, 2018, **24**, 3528–3538.

6 (a) E. I. Tolpin, W. N. Lipscomb, *J. Am. Chem. Soc.*, 1973, **95**, 2384–2386; (b) E. L. Muetterties, E. L. Hoel, C. G. Salentine, M. F. Hawthorne, *Inorg. Chem.*, 1975, **14**, 950–951.

7 (a) A. H. Soloway, W. Tjarks, B. A. Barnum, F.-G. Rong, R. F. Barth, I. M. Codogni, J. G. Wilson, *Chem. Rev.*, 1998, **98**, 1515–1562; (b) N. S. Hosmane, Taylor & Francis Group, Boca Raton, FL, USA, **2012**; (c) M. F. Hawthorne, A. Maderna, *Chem. Rev.*, 1999, **99**, 3421–3434.

8 (a) A. N. Dey, J. Miller, *J. Electrochem. Soc.*, 1979, **126**, 1445–1451; (b) J. W. Johnson, M. S. Whittingham, *J. Electrochem. Soc.*, 1980, **127**, 1653–1654; (c) J. W. Johnson, A. H. Thompson, *J. Electrochem. Soc.*, 1981, **128**, 932–933; (d) J. W. Johnson, J. F. Brody, *J. Electrochem. Soc.*, 1982, **129**, 2213–2219.

9 (a) J. C. Axtell, L. M. A. Saleh, E. A. Qian, A. I. Wixtrom, A. M. Spokoyny, *Inorg. Chem.*, 2018, **57**, 2333–2350; (b) J. Plešek, *Chem. Rev.*, 1992, **92**, 269–278.

10 (a) C. Bolli, J. Derendorf, M. Keßler, C. Knapp, H. Scherer, C. Schulz, J. Warneke, *Angew. Chem. Int. Ed.* **2010**, *49*, 3536–3538; (b) S. V. Ivanov, S. M. Miller, O. P. Anderson, K. A. Solntsev, S. H. Strauss, *J. Am. Chem. Soc.*, 2003, **125**, 4694–4695; (c) M. Kessler, C. Knapp, V. Sagawe, H. Scherer, R. Uzun, *Inorg. Chem.*, 2010, **122**, 5223–5230; (d) A. Avelar, F. S. Tham, C. A. Reed, *3*543–3545; *Angew. Chem., Int. Ed. Engl.* **2009**, *48*, 3491–3493.

11 (a) S. V. Ivanov, J. A. Davis, S. M. Miller, O. P. Anderson, S. H. Strauss, *Inorg. Chem.*, 2003, **42**, 4489–4491; (b) C. Bolli, J. Derendorf, C. Jenne, H. Scherer, C. P. Sindlinger, B. Wegener, *Chem. Eur. J.*, 2014, **20**, 13783–13792.

12 (a) I. M. Riddlestone, A. Kraft, J. Schaefer, I. Krossing, *Angew. Chem. Int. Ed.* **2018**, *57*, DOI: 10.1002/anie.201710782; (b) C. Knapp, in Comprehensive Inorganic Chemistry II, Vol. 1 (Ed.: T. Chivers), 2012, pp. 651–679.

13 M. Wegener, F. Huber, C. Bolli, C. Jenne, S. F. Kirsch, *Chem. Eur. J.*, 2015, **21**, 1328–1336.

14 D. V. Peryshkov, A. A. Popov, S. H. Strauss, *J. Am. Chem. Soc.*, 2010, **132**, 13902–13913.

15 (a) S. V. Ivanov, W. J. Casteel Jr., W. H. Bailey III, Air Products and Chemicals, Inc., US 7,465,517 B2, 2008; (b) W. J. Casteel Jr., S. V. Ivanov, K. Jambunathan, W. H. Bailey III, Air Products and Chemicals, Inc, WO2009/073514, 2009.

16 (a) R. T. Boeré, S. Kacprzak, M. Keßler, C. Knapp, R. Riebau, S. Riedel, T. L. Roemmele, M. Rühle, H. Scherer, S. Weber, *Angew. Chem. Int. Ed.* **2011**, *50*, 549–552; (b) R. T. Boeré, J. Derendorf, C. Jenne, S. Kacprzak, M. Keßler, R. Riebau, S. Riedel, T. L. Roemmele, M. Rühle, H. Scherer, T. Vent-Schmidt, J. Warneke, S. Weber, *Chem. Eur. J.*, 2014, **20**, 4447–4459.

17 (a) H. Zhao, J. Zhou, P. Jena, *Angew. Chem. Int. Ed.* **2016**, *55*, 3704–3708; (b) J. Moon, H. Baek, J. Kim, *Chem. Phys. Lett.*, 2018, **698**, 72–76.

18 K. I. Assaf, M. S. Ural, F. F. Pan, T. Georiev, S. Simova, K. Rissanen, D. Gabel, W. M. Nau, *Angew. Chem. Int. Ed.* **2015**, *54*, 6852–6856.

19 (a) M. J. Lecours, R. A. Marta, V. Steinmetz, N. Keddie, E. Fillion, D. O'Hagan, T. B. McMahon, W. S. Hopkins, *J. Phys. Chem. Lett.*, 2017, **8**, 109–113; (b) J. Warneke, C. Jenne, J. Bernarding, V. A. Azov, M. Plaumann, *Chem. Commun.*, 2016, **52**, 6300–6303.

20 M. Rohdenburg, M. Mayer, M. Grellmann, C. Jenne, T. Borrmann, F. Kleemiss, V. A. Azov, K. R. Asmis, S. Grabowsky, J. Warneke, *Angew. Chem. Int. Ed.* **2017**, *56*, 7980–7985.

21 D. S. Wilbur, M. K. Chyan, D. K. Hamlin, M. A. Perry, *Bioconjugate Chem.*, 2009, 591–602.

22 D. Awad, M. Bartok, F. Mostaghimi, I. Schrader, N. Sudumbrekar, T. Schaffran, C. Jenne, J. Eriksson, M. Winterhalter, J. Fritz, K. Edwards, D. Gabel, *ChemPlusChem*, 2015, **80**, 656–664.

23 P. J. Kueffer, C. A. Maitz, A. A. Khan, S. A. Schuster, N. I. Shlyakhtina, S. S. Jalisatgi, J. D. Brockman, D. W. Nigg, M. F. Hawthorne, *Proc. Natl. Acad. Sci. USA*, 2013, **110**, 6512–6517.

24 (a) M. F. Roll, *J. Mater. Res.*, 2016, **31**, 2736–2748; (b) B. R. S. Hansen, M. Paskevicius, M. Jorgensen, T. R. Jensen, *Chem. Mater.*, 2017, **29**, 3423–3430; (c) J. Warneke, M. E. McBriarty, S. L. Riechers, S. China, M. H. Engelhard, E. Aprà, R. P. Young, N. M. Washton, C. Jenne, G. E. Johnson, J. Laskin, *Nat. Commun.*, 2018, DOI: 10.1038/s41467-41018-04228-41462.

25 A. I. Boldyrev, J. Simons, *J. Phys. Chem.*, 1994, **98**, 2298–2300.

26 (a) M. K. Scheller, R. N. Compton, L. S. Cederbaum, *Science*, 1995, **270**, 1160–1166; (b) L. S. Wang, C. F. Ding, X. B. Wang, J. B. Nicholas, B. Nicholas, *Phys. Rev. Lett.*, 1998, **81**, 2667–2670; (c) J. Simons, P. Skurski, R. Barrios, *J. Am. Chem. Soc.*, 2000, **122**, 11893–11899; (d) A. Dreuw, L. S. Cederbaum, *Chem. Rev.*, 2002, **102**, 181–200; (e) W. E. Boxford, C. E. H. Dessent, *Phys. Chem. Chem. Phys.*, 2006, **8**, 5151–5165; (f) X. B. Wang, H. K. Woo, X. Huang, M. M. Kappes, L. S. Wang, *Phys. Rev. Lett.*, 2006, **96**, 143002; (g) J. R. R. Verlet, D. A. Horke, A. S. Chatterley, *Phys. Chem. Chem. Phys.*, 2014, **16**, 15043–15052.

27 M. L. McKee, Z. X. Wang, P. V. Schleyer, *J. Am. Chem. Soc.*, 2000, **122**, 4781–4793.

28 (a) A. Dreuw, N. Zint, L. S. Cederbaum, *J. Am. Chem. Soc.*, 2002, **124**, 10903–10910; (b) N. Zint, A. Dreuw, L. S. Cederbaum, *J. Am. Chem. Soc.*, 2002, **124**, 4910–4917; (c) M. Zhong, J. Zhou, H. Fang, P. Jena, *Phys. Chem. Chem. Phys.*, 2017, **19**, 17937–17943.

29 J. Warneke, G.-L. Hou, E. Aprà, C. Jenne, Z. Yang, Z. Qin, K. Kowalski, X.-B. Wang, S. S. Xantheas, *J. Am. Chem. Soc.*, 2017, **139**, 14749–14756.

30 (a) V. Geis, K. Guttsche, C. Knapp, H. Scherer, R. Uzun, *Dalton Trans.*, 2009, 2687–2694; (b) E. V. Bukovsky, D. V. Peryshkov, H. Wu, W. Zhou, W. S. Tang, W. M. Jones, V. Stavila, T. J. Udovic, S. H. Strauss, *Inorg. Chem.*, 2017, **56**, 4369–4379.

31 S. V. Ivanov, S. M. Ivanova, S. M. Miller, O. P. Anderson, K. A. Solntsev, S. H. Strauss, *Inorg. Chem.*, 1996, **35**, 6914.
32 M. Finze, *Angew. Chem. Int. Ed.* **2007**, *46*, 8880-8882.
33 (a) D. S. Wilbur, M.-K. Chyan, D. K. Hamlin, B. B. Kegley, R. Risler, P. M. Pathare, J. Quinn, R. L. Vessella, C. Foulon, M. Zalutsky, T. J. Wedge, M. F. Hawthorne, *Bioconjugate Chem.*, 2004, **15**, 203–223; (b) J. Ruiz-Cabello, B. P. Barnett, P. A. Bottomley, J. W. M. Bulte, *NMR Biomed.*, 2011, **24**, 114–129.
34 J. Warneke, T. Dülcks, C. Knapp, D. Gabel, *Phys. Chem. Chem. Phys.*, 2011, **13**, 5712–5721.
35 (a) P. Farras, N. Vankova, L. L. Zeonjuk, J. Warneke, T. Dülcks, T. Heine, C. Viñas, F. Teixidor, D. Gabel, *Chem. Eur. J.*, 2012, **18**, 13208–13212; (b) M. R. Fagiani, L. L. Zeonjuk, T. K. Esser, D. Gabel, T. Heine, K. R. Asmis, J. Warneke, *Chem. Phys. Lett.*, 2015, **625**, 48–52; (c) L.-F. Gong, W. Li, E. Osorio, X.-M. Wu, T. Heine, L. Liu, *J. Chem. Phys.*, 2017, **147**, 144302.
36 (a) H. J. Zhai, B. Kiran, J. Li, L. S. Wang, *Nat. Mater.*, 2003, **2**, 827–833; (b) I. Boustani, *Chem. Phys. Lett.*, 1995, **240**, 135–140.
37 (a) Z. A. Piazza, I. A. Popov, W. L. Li, R. Pal, X. C. Zeng, A. I. Boldyrev, L. S. Wang, *J. Chem. Phys.*, 2014, **141**, 034303; (b) S. Jalife, L. Liu, S. Pan, J. L. Cabellos, E. Osorio, C. Lu, T. Heine, K. J. Donald, G. Merino, *Nanoscale*, 2016, **8**, 17639–17644; (c) M. R. Fagiani, X. W. Song, P. Petkov, S. Debnath, S. Gewinner, W. Schöllkopf, T. Heine, A. Fielicke, K. R. Asmis, *Angew. Chem. Int. Ed.* **2017**, *56*, 501–504; (d) Y. G. Yang, D. M. Jia, Y. J. Wang, H. J. Zhai, Y. Man, S. D. Li, *Nanoscale*, 2017, **9**, 1443–1448.
38 V. V. Avdeeva, E. A. Malinina, I. B. Sivaev, V. I. Bregadze, N. T. Kuznetsov, *Crystals*, 2016, **6**, 60; doi:10.3390/cryst6050060.
39 W. S. Hopkins, P. J. J. Carr, D. Huang, K. P. Bishop, M. Burt, T. B. McMahon, V. Steinmetz, E. Fillion, *J. Phys. Chem. A*, 2015, **119**, 8469–8475.
40 C. Jenne, M. Keßler, J. Warneke, *Chem. Eur. J.*, 2015, **21**, 5887–5891.
41 O. Volkov, P. Paetzold, C. Hu, U. Kölle, *Z. Anorg. Allg. Chem.*, 2001, **627**, 1029–1033.
42 (a) W. Einholz, K. Vaas, C. Wieloch, B. Speiser, T. Wizemann, M. Ströbele, H.-J. Meyer, *Z. Anorg. Allg. Chem.*, 2002, **628**, 258–268; (b) J. Holub, S. El Anwar, T. Jelínek, L. Fojt, Z. Růžičková, V. Šolínová, V. Kašička, D. Gabel, B. Grüner, *Eur. J. Inorg. Chem.*, 2017, 4499–4509; (c) W. H. Knoth, H. C. Miller, J. C. Sauer, J. H. Balthis, Y. T. Chia, E. L. Muetterties, *Inorg. Chem.*, 1964, **3**, 159–167.
43 E. Bernhardt, H. Willner, Bergische Universität Wuppertal, DE102008004530A1, 2009.
44 E. L. Klanberg, E. L. Muetterties, *Inorg. Synth.*, 1968, **XI**, 25–27.
45 O. Volkov, K. Radacki, P. Paetzold, X. Zheng, *Z. Anorg. Allg. Chem.*, 2001, **627**, 1185–1191.
46 I. Tiritiris, T. Schleid, *Z. Anorg. Allg. Chem.*, 2004, **630**, 1555–1563.
47 (a) K. A. Solntsev, A. M. Mebel', N. A. Votinova, N. T. Kuznetsov, O. P. Charkin, *Koord. Khim.*, 1992, **18**, 340; (b) D. V. Peryshkov, A. A. Popov, S. H. Strauss, *J. Am. Chem. Soc.*, 2009, **131**, 18393–18403.
48 E. V. Bukovsky, A. M. Pluntze, S. H. Strauss, *J. Fluorine Chem.*, 2018, **203**, 90–98.
49 K. A. Solntsev, S. V. Ivanov, S. G. Sakharov, S. B. Katser, A. S. Chernyavskii, N. A. Votinova, E. A. Klyuchishche, N. T. Kuznetsov, *Russ. J. Coord. Chem.*, 1997, **23**, 369–376.
50 S. Z. Konieczka, M. Drisch, F. Keppner, M. Finze, *unpublished results*.
51 (a) S. V. Ivanov, S. M. Ivanova, S. M. Miller, O. P. Anderson, N. T. Kuznetsov, K. A. Solntsev, S. H. Strauss, *Collect. Czech. Chem. Commun.*, 1997, **62**, 1310–1324; (b) S. V. Ivanov, A. J. Lupinetti, K. A. Solntsev, S. H. Strauss, *J. Fluorine Chem.*, 1998, **89**, 65–72.
52 M. Finze, G. J. Reiss, *Eur. J. Inorg. Chem.*, 2008, 2321–2325.
53 X. B. Wang, L. S. Wang, *Rev. Sci. Instrum.*, 2008, **79**, 073108.
54 D. Hanstorp, M. Gustafsson, *J. Phys. Chem. B*, 1992, **25**, 1773–1783.
55 X.-B. Wang, L.-S. Wang, *J. Chem. Phys.*, 1999, **111**, 4497–4509.
56 M. Valiev, E. J. Bylaska, N. Govind, K. Kowalski, T. P. Straatsma, H. J. J. Van Dam, D. Wang, J. Niepolcha, E. Apra, T. L. Windus, W. A. de Jong, *Comput. Phys. Commun.*, 2010, **181**, 1477–1489.
57 C. Adamo, V. Barone, *J. Chem. Phys.*, 1999, **110**, 6158–6170.
58 (a) T. H. Dunning Jr., *J. Chem. Phys.*, 1989, **90**, 1007–1023; (b) D. E. Woon, T. H. Dunning Jr., *J. Chem. Phys.*, 1993, **98**, 1358–1371; (c) A. K. Wilson, D. E. Woon, K. A. Peterson, T. H. Dunning Jr., *J. Chem. Phys.*, 1999, **110**, 7667–7676; (d) K. A. Peterson, D. Figgen, E. Goll, H. Stoll, M. Dolg, *J. Chem. Phys.*, 2003, **119**, 11113–11123.
59 D. Rappoport, F. Furche, *J. Chem. Phys.*, 2010, **133**, 134105.
60 S. Grimme, J. Antony, S. Ehrlich, H. Krieg, *J. Chem. Phys.*, 2010, **132**, 154104.

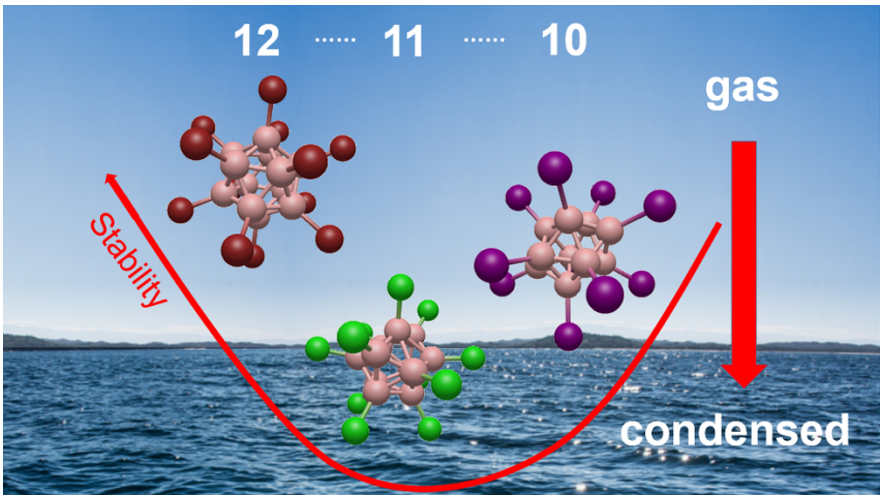

A comparative study of the trends of the electronic properties and reactivity of *closo*-borates $[closo\text{-}B_nX_n]^{2-}$ (X = halogen) along the parameters cluster size (n = 10, 11, 12) and halogen substituent (X = F, Cl, Br, I) was undertaken that connects gas and condensed phase properties.